Annals of Anatomy 223 (2019) 43–48

Contents lists available at ScienceDirect

Annals of Anatomy

journal homepage: www.elsevier.com/locate/aanat

RESEARCH ARTICLE

Altered laryngeal morphology in *Period1* deficient mice

Olaf Bahlmann[a,*,1], Christoph Schürmann[b,1], Erik Maronde[a]

[a] Dr. Senckenbergische Anatomie, Institute of Anatomy III, Goethe University Frankfurt, 60590 Frankfurt am Main, Germany
[b] Institute for Cardiovascular Physiology, Goethe University Frankfurt, Theodor-Stern-Kai 7, 60596 Frankfurt am Main, Germany

ARTICLE INFO

Article history:
Received 8 November 2018
Received in revised form 14 January 2019
Accepted 14 January 2019

Keywords:
Ultrasonic vocalizations
Mouse
Larynx
Cartilage
Micro-computed-tomography
Stereology

ABSTRACT

Background: Ultrasonic vocalizations (USV) of mice are produced in and emitted by the larynx. However, which anatomical elements of the mouse larynx are involved and to which aspects of USV they contribute is not clear.

Frequency and amplitude parameters of mice, deficient in the clock gene *Period1* (*mPer1*$^{-/-}$ mice) are distinguishably different compared to C3H wildtype (WT) controls. Because structural differences in the larynx may be a reason for the different USV observed, we analyzed laryngeal anatomy of *mPer1*$^{-/-}$ mice and WT control animals using micro-computed-tomography and stereology.

Results: In *mPer1*$^{-/-}$ mice, we found laryngeal cartilages to be normally arranged, and the thyroid, arytenoid and epiglottal cartilages were similar in diameter and volume measurements, compared to WT mice. However, in the cricoid cartilage, a significant difference in the dorso-ventral diameter and volume was evident.

Conclusion: Our findings imply that laryngeal morphology is affected by inactivation of the clock gene *Period1* in mice, which may contribute to their abnormal USV.

1. Introduction

The vertebrate larynx evolved from a simple sphincter that protects the lower airways to a complex structure with protective, respiratory and phonatory function (Harrison, 2009; Paulsen, 1967). Though laryngeal morphology varies between species, the basic anatomy is preserved in mammals (Harrison, 2009).

1.1. Anatomy of the larynx

The larynx belongs to the upper respiratory tract. Its primary function is protection of the airways from aspiration of particles and food. The laryngeal cavity contains the laryngeal vestibule, the glottis with the vocal folds, and the infraglottal cavity. The laryngeal skeleton is composed of three paired and three unpaired cartilages. The skeletal elements are connected by joints, ligaments and membranes (Harrison, 2009; Paulsen, 1967). Intrinsic laryngeal muscles open and close the vocal folds and regulate their tension (Harrison, 2009).

Although the principle rodent (murine) laryngeal framework is similar to the human larynx, there are anatomical variations. Compared to humans, a structure unique to some rodents including mice and rats is the ventral pouch or sac, which bulges ventrally, cranial to the vocal cords. Also a U-shaped alar cartilage is positioned at the entrance of the ventral pouch (Alli et al., 2013; Inagi et al., 2016; Riede et al., 2017; Sagartz et al., 1992; Thomas et al., 2009) present in rats (Sagartz et al., 1992; Thomas et al., 2009) and mice (Sagartz et al., 1992; Thomas et al., 2009) and presumably other small rodents.

1.2. Sound production in mammals

In mammals, vocal folds serve the larynx for sound production. Thereby, the adducted vocal folds are set into vibration by an airstream from the lung. The vocalization tract spans from the larynx to the lips. However, the spectrum of sound production of mammals is diverse, with e.g. ultrasonic sounds in bats or infrasonic sound production in whales (Fitch and Hauser, 2003).

The acoustic frequency range, i.e. the frequencies humans perceive, span from 20 Hz to 20 kHz. Frequencies below or above this range are called infra- and ultrasonic sounds, respectively. USV are produced by rats, mice and other rodents, and some whales and bats. USV are used for echolocation, navigation, and prey capture.

* Corresponding author.
E-mail address: bahlmann@med.uni-frankfurt.de (O. Bahlmann).
[1] Equal first authors.

https://doi.org/10.1016/j.aanat.2019.01.009
0940-9602/

They also serve for social interaction, which is well investigated in rats and mice (Harrison, 2009; Roberts, 1975a).

Rodents vocalize with frequencies both audible and not audible (USV) for humans. The sounds rodents produce span five octaves and the USV range up to 110 kHz. The upper frequency hearing limit of rodents is higher than the human limit (Heckman et al., 2016; Heffner and Heffner, 2007). Zippelius and Schleidt recognized emitted sounds between 70 and 80 kHz in a young mouse under discomforting conditions like cooling and touching (Zippelius and Schleidt, 1956). Indeed, fostering mouse mothers and fathers react to new-born USV with approaching and caring behaviour (Liu et al., 2013). USV are also an integral part of rodent courtship behaviour (Hammerschmidt et al., 2009; Wöhr and Schwarting, 2010). Besides the behavioural state, the genetic background (mouse strain), age and gender affect USV (Arriaga and Jarvis, 2013; Barnes et al., 2016; Heckman et al., 2016). Mouse models of various types of neurological disorders, e.g., Forkhead-Box-Protein P2 (FOXP2) related language and speech disorders, show specific patterns of USV (Scattoni et al., 2009).

1.3. Aim of the present study

A study on USV emitted by new-born mice deficient in the clock gene *period1* (*mPer1*$^{-/-}$ mice) while separated from their mothers (pup isolation calls) and by adult male *mPer1*$^{-/-}$ mice confronted with a female (female induced male USV) showed altered frequency and amplitude parameters, compared to WT controls. Compared to WT mice, *mPer1*$^{-/-}$ mice showed a trend towards lower frequency in USV calling and mean peak amplitude was significantly higher at day 10 (Bechstein et al., 2014). Based on this work, we investigated in the present study the morphology of the laryngeal skeleton, which may help to explain the differences in USV call parameters.

2. Materials and methods

2.1. *Per1*$^{-/-}$ and wildtype mice

Per1$^{-/-}$ and wildtype C3H/HeN mice (WT) were sacrificed at 12 weeks of age. Perfusion fixation was carried out as described previously (Jilg et al., 2010).

2.2. Ex vivo *micro-CT*

Specimens were immersed overnight in 4% PFA and subsequently scanned in the micro-CT (Skyscan 1176, Bruker micro-CT, Kontich, Belgium) with the following settings: 50 kV, 0.5 mm aluminium filter, 500 μA source current, exposure time 875 ms, 9 μm isotopic resolution, 7 projection images per 0.3° rotation step, rotation range 180° and a field of view (FOV) covering the entire neck.

Volumetric data was reconstructed with the NRecon/InstaRecon CBR Server — Premium software (Skyscan, Kontich, Belgium/InstaRecon, Champaign, Illinois, USA). Image analysis, segmentation of micro-CT data and quantification of vocal tract length (VTL), thyroid and cricoid cartilage were performed with the Imalytics Preclinical Software (Gremse-IT, Aachen, Germany) (Gremse et al., 2016). Discrimination of calcified cartilage and bone was achieved by applying fixed thresholds. Landmarks for the vocal tract length were chosen as described elsewhere (Inagaki et al., 2012). Briefly, the VTL was measured between the tip of the nose and the rostral edge of the thyroid cartilage. Illustration was performed with Imaris Imalytics or Syngo.via Cinematic Rendering (Siemens, Erlangen, Germany).

2.3. Histology and stereology

After micro-CT investigation, specimens were stored in 70% isopropanol and further dissected for morphological investigation. The dissected larynx specimens were consecutively immersed in 15% and 30% sucrose for one day and finally placed in O.C.T. Compound (Tissue Tek, Hartenstein, Würzburg, Germany). Afterwards, specimens were positioned in a freezing mould. The mould was filled with O.C.T. and frozen on dry ice. The frozen block was sectioned at 12 μm and every tenth section was harvested. Sections were stained with Haematoxylin.

Micrographs of the sections were taken with a Neofluar 1.25/0.035 ocular lens (Zeiss, Oberkochen, Germany). Images were loaded into ImageJ (Schindelin et al., 2012). For stereology, the image contrast was enhanced, a point grid was overlaid and test points on cartilage tissue counted. The volume of the laryngeal cartilages was estimated by the number of points multiplied with the area per point and the distance between sections (Yoruk et al., 2009).

For 3D inspection of laryngeal anatomy, in a WT larynx, the cartilages were manually segmented and the larynx was reconstructed in Fiji/ImageJ Volume Viewer (Schindelin et al., 2012) (Plugin: http://imagej.net/plugins/volume-viewer.html).

2.4. Statistical analysis

Statistical analyses were performed by Studentś t-test. Values of $p < 0.05$ were considered statistically significant (GraphPad Prism, La Jolla, USA).

3. Results

3.1. Ex vivo *micro-CT*

Micro-CT enabled visualization of the hyoid bone, thyroid and cricoid cartilage (Fig. 1a–c). Arytenoid and epiglottal cartilage could not be visualized by micro-CT. VTL, measured between the tip of the nose and the rostral edge of the thyroid cartilage, was not significantly different between *mPer1*$^{-/-}$ and WT mice (Fig. 2a). Micro-CT enabled diameter quantification of calcified thyroid and cricoid cartilage (Fig. 2B–D). In WT and *mPer1*$^{-/-}$ mice, the thyroid and cricoid cartilage diameter (right-left) did not differ between both mouse genotypes. However, micro-CT revealed a significantly reduced dorso-ventral diameter of the cricoid cartilage in *mPer1*$^{-/-}$, compared to WT animals (Fig. 2d).

3.2. Histology and stereology

Random sectioning of the laryngeal skeleton started at the level of the uppermost tracheal ring. The serial sections covered the dorsal plate of the cricoid cartilage. This cartilage formed a ring and articulated with the thyroid cartilage. The following sections showed the typical horseshoe shape of the thyroid. Further sectioning covered the arytenoid cartilages and ended just after the top of the epiglottis, at the beginning of the palate. In the larynx sections, basic anatomy of the laryngeal skeleton was the same for *mPer1*$^{-/-}$ and WT mice (Figs. 3 and 4).

In the stereological analysis, there were no significant differences in the thyroid, arytenoid and epiglottal cartilage volume estimates. The stereological volume estimate of the cricoid cartilage, on the contrary, was significantly larger in *mPer1*$^{-/-}$ mice, compared to WT mice ($p < 0.05$) (Fig. 3a–d).

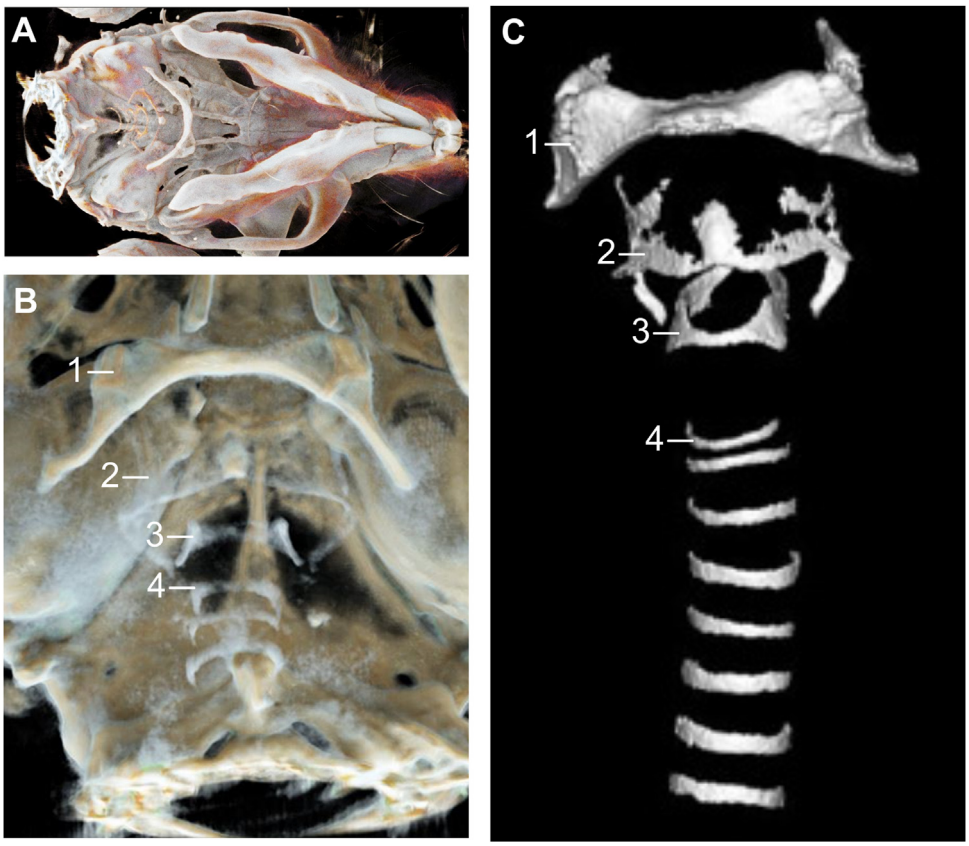

Fig. 1. Micro-CT imaging of the murine skull and larynx.
(A) and (B) Volume rendering of the skull and larynx in a WT mouse using Cinematic Rendering. (C) Segmented laryngeal skeleton and allocation of laryngeal cartilages using Imalytics Preclinical. (1) Hyoid bone, (2) thyroid cartilage, (3) cricoid cartilage, (4) tracheal ring(s).

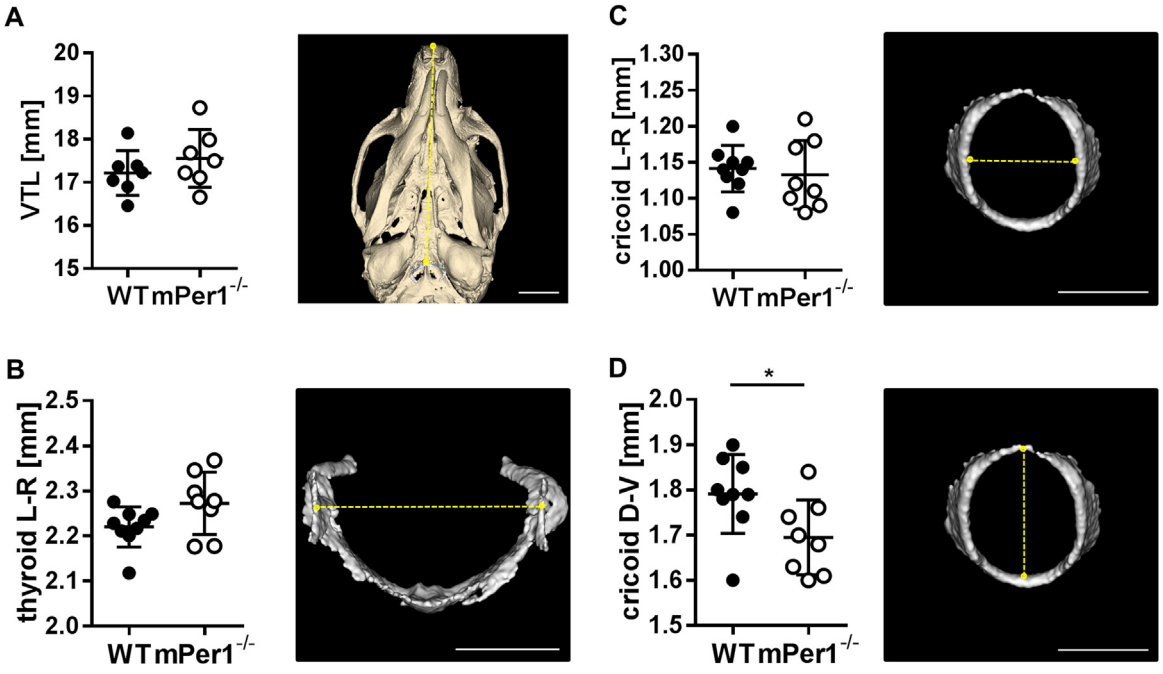

Fig. 2. Quantification of vocal tract length and laryngeal diameters in micro-CT.
(A) Vocal tract length (WT: N = 7; *mPer1*$^{-/-}$: N = 7), measured from tip of the nose to the rostral edge of the thyroid cartilage in a WT mouse. (B–D) Segmentation of the thyroid and cricoid cartilage (WT: N = 9; *mPer1*$^{-/-}$: N = 8). Measures of cartilaginous diameters depicted with dashed lines. The statistical comparison showed that the dorso-ventral (D–V) diameter of the cricoid cartilage was smaller in *mPer1*$^{-/-}$ mice, compared to controls ($p < 0.05$). Data are shown with mean and standard deviation. Scale bar in (A) 2.5 mm and (B–D) 1 mm.

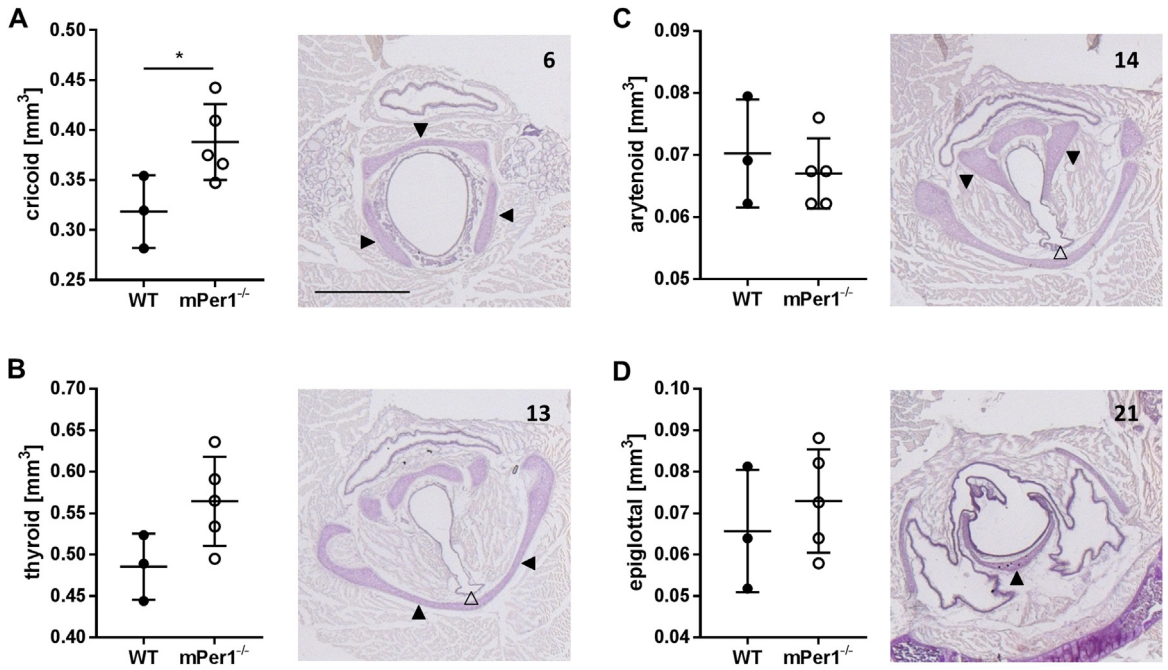

Fig. 3. Stereology of the larynx.
Volume of the cricoid (A), thyroid (B), arytenoid (C) and epiglottal cartilage (D) with corresponding exemplary histological cross sections in a WT mouse (WT: N = 3; *mPer1*$^{-/-}$: N = 5). The numbers indicate the position in a series of 26 sections through the larynx from caudal to cranial. The corresponding cartilage, depicted by filled arrows, is shown in its largest extend. The ventral sac out pouches the laryngeal lumen in (B) and (C) (open arrow). In the statistical analysis, the volume estimate of the cricoid cartilage was larger, compared to control mice ($p < 0.05$). Data are shown with mean and standard deviation. Scale bar 1 mm.

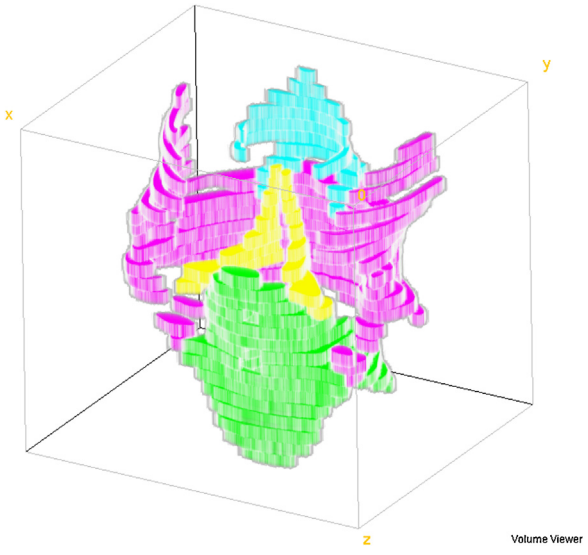

Fig. 4. Volume reconstruction of the larynx.
Manual segmentation and reconstruction of 26 histological cross-sections through the larynx in a WT mouse. Images were segmented, coloured and aligned in Adobe Photoshop CS and loaded in Fiji/ImageJ Volume Viewer (Plugin: http://imagej.net/plugins/volume-viewer.html). Dorsal view on the cricoid in green, thyroid in red, arytenoid in yellow and epiglottal cartilage in cyan. (For interpretation of the references to colour in this figure legend, the reader is referred to the web version of this article).

4. Discussion

In this study, we found that the basic anatomy of the larynx of *mPer1*$^{-/-}$ was similar to WT mice. However, micro-CT and stereology displayed a smaller dorso-ventral diameter and a larger volume of the cricoid cartilage in *mPer1*$^{-/-}$ mice, compared to WT controls.

4.1. Limitations

Micro-CT is mostly used to image bone tissue (Clark and Badea, 2014). In contrast, imaging non-calcified soft tissue is difficult because it yields low contrast (Clark and Badea, 2014). Thus, in a study on the larynx of several rodent species, the tissue was iodinated for 13–17 days before scanning (Riede et al., 2017), a technique known to produce higher contrast in soft tissues (Clark and Badea, 2014). In the present study, using a test specimen, we evaluated iodination, but we were not able to increase the contrast in the tissue. Though we tried various threshold values in the segmentation process, we were unable to visualize the arytenoid cartilages and the epiglottis. However, in the histological analysis, all laryngeal cartilages could be investigated.

4.2. Laryngeal morphology in mPer1$^{-/-}$ mice

Laryngeal dimensions significantly influence the production of voiced sounds. For instance, there are differences between females and males in average fundamental frequency correlating with laryngeal size. The length and shape of the vocal tract are also crucial for the production of formant frequencies (Harrison, 2009). Apart from voiced sounds, laryngeal dimensions will also affect USV in the mouse.

In rodents, early studies identified the larynx as the source of USV (Riede, 2011; Riede et al., 2017; Roberts, 1975a). Frequency recordings of rodents in air and light gases (heliox) suggested that the mechanism for USV production must be different from the way voiced sounds are produced by vibrating vocal folds, hence, a hole-tone (birdcall) mechanism was proposed (Roberts, 1975a, 1975b; 1975c). In a hole-tone mechanism, an air jet leaves a circular opening and travels through a second hole downstream (Dornfeld, 2017). The first opening is likely formed by the glottis (Johnson et al., 2010; Sanders et al., 2001). An aperture formed by the tongue pressed against the palate or, alternatively, the epiglottis in a semi-

opened position could provide the second opening (Brudzynski and Fletcher, 2010). However, some recent experiments in heliox challenged the hole-tone whistle mechanism for USV sound production (Berquist, 2013; Riede, 2011). Applied to our results, a reduced dorso-ventral diameter of the cricoid in *mPer1*$^{-/-}$ mice might approximate the two openings and thereby affect the USV pattern.

Recently, alternative mechanisms for USV production were proposed. In the intralaryngeal planar-impinging-air-jet model, USV are produced by an air jet impinging on a planar plane formed by the thyroid cartilage or parts of the epiglottis, in conjunction with a feedback mechanism. (Mahrt et al., 2016). Transferred to our findings, the altered laryngeal morphology in *mPer1*$^{-/-}$ mice might change the impingement length and contribute to the aberrant frequency parameters observed in *mPer1*$^{-/-}$ mice (Bechstein et al., 2014).

In the edge-tone model, an air jet released through the glottis is directed at the alar edge of the ventral pouch, which results in an undulating flow. In this model, constriction of the alar portion of the thyroarytenoid muscle might change the distance between the glottis and the alar edge and the size of the ventral pouch, and thereby affect the frequency of USV (Riede et al., 2017).

We determined the pouch volume in the two, respectively three sections per specimen that showed cross sections of the alar cartilage (partial pouch volume), and we did not find a significant difference (data not shown).

In previous studies, whole body size and weight were reported to be reduced in *mPer1*$^{-/-}$ compared to WT mice (Bae et al., 2006; Bechstein et al., 2014; Pilorz and Steinlechner, 2008). However, smaller sized *mPer1*$^{-/-}$ mice do not show a smaller larynx. In fact, the cricoid's volume is significantly larger, compared to WT mice. These findings show that the larynx in *mPer1*$^{-/-}$ mice is relatively large in relation to whole body size and weight, which also might contribute to differences in USV patterns compared to WT mice.

4.3. Per1 *in bone and cartilage tissue*

Several gene/protein networks involved in laryngeal or tracheal skeletal development are up- or downregulated in previously gathered microarray data of *mPer1*$^{-/-}$ and WT mice (Jilg et al., 2010; Rawashdeh et al., 2014, 2016) (for details see Supplemental Table 1). These are antagonists of the ß-catenin pathway (*Dact1,2*), genes of the Fgf/Fgfr family (*Fgf1,2* and *16*; *Fgfr1,2* and *3*), signal transducer and activator of transcription 3 (*Stat3*) and genes associated with the wingless pathway (*Wnt3*, *9b*, *10b* and *Wisp*). *Per1* is involved in the development, maintenance and remodeling of bone tissue. E.g., in a study on bone mineral density (BMD) in women, *Per1* polymorphisms were associated with BMD in the lower lumbar spine (Kim et al., 2014). *Per1* is also involved in the biology of cartilage tissue (Yang and Meng, 2016). In a pre-chondrogenic cell line, *Per1* was transiently upregulated by parathyroid hormone treatment (Hinoi et al., 2006). Clock genes are also involved in gene expression in the cartilaginous rib growth plate, where they affect enchondral ossification (Takarada et al., 2017). However, in a study on the effect of clock genes on bone formation, bone morphometric parameters in the skeletal system of *Per1*$^{-/-}$ mice did not differ significantly from WT animals (Maronde et al., 2010). Above mentioned differentially regulated genes might be candidates to start with in a further study on the molecular mechanisms behind the influence of *Per1* on (laryngeal) cartilage tissue.

Per1 is also expressed in epithelium and submucosal glands of the larynx (Bando et al., 2007; Nishio et al., 2008). However, we did not find published work on the expression of *Per1* in laryngeal cartilage tissue. Apart from its effect on laryngeal morphology in the mouse, it would be interesting to investigate the role of *Per1* in the human larynx, because *Per1* is discussed in aging processes (Pilorz et al., 2009), and aging of the human larynx is well documented showing a progressive ossification of the cartilage tissue in elderly subjects (Claassen et al., 2014).

5. Conclusion

In conclusion, our results imply that inactivation of the clock gene *Period1* influences laryngeal morphology, which might contribute to the abnormal USV patterns previously observed in *mPer1*$^{-/-}$ mice. Microarray data helped us to identify genes which are differentially regulated in *mPer1*$^{-/-}$ and WT mice and which are known to be involved in laryngeal development. Further studies might reveal whether *Per1* signaling in the murine larynx interacts molecularly with some of these genes.

Authors' contributions

EM conceived the study. EM and CS designed and coordinated the study. CS carried out the micro-CT and OB carried out the histology and stereology. CS and OB analyzed the data and all authors helped drafting the manuscript. All authors gave final approval for publication.

Funding

The study was supported by the Faculty of Medicine, Goethe University Frankfurt, Frankfurt am Main, Germany and the German Center for Cardiovascular Research (DZHK), Partner site RheinMain, Frankfurt am Main, Germany (CS).

Ethical statement

Experiments were conducted in accordance to the guidelines of the European Communities Council Directive (89/ 609/EEC) for humane animal care.

Acknowledgements

We thank Jörg Stehle for valuable contributions to the manuscript and together with Ralf Brandes for continuous support, Klaus Engel for the illustration using syngo.via Cinematic Rendering (Siemens, Erlangen, Germany). EM wants to dedicate this work to two pioneers of mammalian USV research, Wolfgang Schleidt and Gillian Sales.

Appendix A. Supplementary data

Supplementary material related to this article can be found, in the online version, at doi:https://doi.org/10.1016/j.aanat.2019.01.009.

References

Alli, O., Berzofsky, C., Sharma, S., Pitman, M.J., 2013. Development of the rat larynx: a histological study. Laryngoscope 123, 3093–3098, http://dx.doi.org/10.1002/lary.24145.

Arriaga, G., Jarvis, E.D., 2013. Mouse vocal communication system: are ultrasounds learned or innate? Brain Lang. 124, 96–116, http://dx.doi.org/10.1016/j.bandl.2012.10.002.

Bae, K., Lee, K., Seo, Y., Lee, H., Kim, D., Choi, I., 2006. Differential effects of two period genes on the physiology and proteomic profiles of mouse anterior tibialis muscles. Mol. Cells 22, 275–284.

Bando, H.H., Nishio, T.T., van der Horst, G.T.J.G., Masubuchi, S.S., Hisa, Y.Y., Okamura, H.H., 2007. Vagal regulation of respiratory clocks in mice. J. Neurosci. 27, 4359–4365, http://dx.doi.org/10.1523/JNEUROSCI.4131-06.2007.

Barnes, T.D., Wozniak, D.F., Gutierrez, J., Han, T.-U., Drayna, D., Holy, T.E., 2016. A mutation associated with stuttering alters mouse pup ultrasonic vocalizations. Curr. Biol. 26, 1009–1018, http://dx.doi.org/10.1016/j.cub.2016.02.068.

Bechstein, P., Rehbach, N.-J., Yuhasingham, G., Schürmann, C., Göpfert, M., Kössl, M., Maronde, E., 2014. The clock gene Period1 regulates innate routine behaviour in mice. Proc. R. Soc. B Biol. Sci. 281, http://dx.doi.org/10.1098/rspb.2014.0034, 20140034–20140034.

Berquist, S., 2013. Sound Production in the Isolated Mouse Larynx (Master of Science Thesis). UCLA.

Brudzynski, S.M., Fletcher, N.H., 2010. Rat ultrasonic vocalization: short-range communication. Handb. Behav. Neurosci. 19, 69–76, http://dx.doi.org/10.1016/B978-0-12-374593-4.00008-5.

Claassen, H., Schicht, M., Sel, S., Paulsen, F., 2014. Special pattern of endochondral ossification in human laryngeal cartilages: X-ray and light-microscopic studies on thyroid cartilage. Clin. Anat. 27, 423–430, http://dx.doi.org/10.1002/ca.22309.

Clark, D.P., Badea, C.T., 2014. Micro-CT of rodents: state-of-the-art and future perspectives. Phys. Med. Eur. J. Med. Phys. 30, 619–634, http://dx.doi.org/10.1016/j.ejmp.2014.05.011.

Dornfeld, M., 2017. The Physics of Rodent Ultrasonic Vocalizations. Student Theses and Dissertations. Rockefeller University, pp. 400.

Fitch, W.T., Hauser, M.D., 2003. Unpacking "honesty": vertebrate vocal production and the evolution of acoustic signals. In: Acoustic Communication, Springer Handbook of Auditory Research. Springer, New York, NY, New York, pp. 65–137, http://dx.doi.org/10.1007/0-387-22762-8_3.

Gremse, F., Stärk, M., Ehling, J., Menzel, J.R., Lammers, T., Kiessling, F., 2016. Imalytics preclinical: interactive analysis of biomedical volume data. Theranostics 6, 328–341, http://dx.doi.org/10.7150/thno.13624.

Hammerschmidt, K., Radyushkin, K., Ehrenreich, H., Fischer, J., 2009. Female mice respond to male ultrasonic "songs" with approach behaviour. Biol. Lett. 5, 589–592, http://dx.doi.org/10.1098/rsbl.2009.0317.

Harrison, D.F.N., 2009. The Anatomy and Physiology of the Mammalian Larynx. Cambridge University Press, Cambridge, http://dx.doi.org/10.1017/CBO9780511525766.

Heckman, J., McGuinness, B., Celikel, T., Englitz, B., 2016. Determinants of the mouse ultrasonic vocal structure and repertoire. Neurosci. Biobehav. Rev. 65, 313–325, http://dx.doi.org/10.1016/j.neubiorev.2016.03.029.

Heffner, H.E., Heffner, R.S., 2007. Hearing ranges of laboratory animals. J. Am. Assoc. Lab. Anim. Sci. 46, 20–22.

Hinoi, E., Ueshima, T., Hojo, H., Iemata, M., Takarada, T., Yoneda, Y., 2006. Up-regulation of per mRNA expression by parathyroid hormone through a protein kinase a-CREB-dependent mechanism in chondrocytes. J. Biol. Chem. 281, 23632–23642, http://dx.doi.org/10.1074/jbc.M512362200.

Inagaki, H.H., Takeuchi, Y.Y., Mori, Y.Y., 2012. Close relationship between the frequency of 22-kHz calls and vocal tract length in male rats. Physiol. Behav. 106, 224–228, http://dx.doi.org/10.1016/j.physbeh.2012.01.018.

Inagi, K., Schultz, E., Ford, C.N., 2016. An anatomic study of the rat larynx: establishing the rat model for neuromuscular function. Otolaryngol Head Neck Surg 118, 74–81, http://dx.doi.org/10.1016/S0194-5998(98)70378-X.

Jilg, A., Lesny, S., Peruzki, N., Schwegler, H., Selbach, O., Dehghani, F., Stehle, J.H., 2010. Temporal dynamics of mouse hippocampal clock gene expression support memory processing. Hippocampus 20, 377–388, http://dx.doi.org/10.1002/hipo.20637.

Johnson, A.M., Ciucci, M.R., Russell, J.A., Hammer, M.J., Connor, N.P., 2010. Ultrasonic output from the excised rat larynx. J. Acoust. Soc. Am. 128, EL75–EL79, http://dx.doi.org/10.1121/1.3462234.

Kim, H., Koh, H., Ku, S.-Y., Kim, S.H., Kim, J.H., Kim, J.G., 2014. Association between polymorphisms in period genes and bone density in postmenopausal korean women. Climacteric 17, 605–612, http://dx.doi.org/10.3109/13697137.2014.905527.

Liu, H.-X., Lopatina, O., Higashida, C., Fujimoto, H., Akther, S., Inzhutova, A., Liang, M., Zhong, J., Tsuji, T., Yoshihara, T., Sumi, K., Ishiyama, M., Ma, W.-J., Ozaki, M., Yagitani, S., Yokoyama, S., Mukaida, N., Sakurai, T., Hori, O., Yoshioka, K., Hirao, A., Kato, Y., Ishihara, K., Kato, I., Okamoto, H., Cherepanov, S.M., Salmina, A.B., Hirai, H., Asano, M., Brown, D.A., Nagano, I., Higashida, H., 2013. Displays of paternal mouse pup retrieval following communicative interaction with maternal mates. Nat. Commun. 4, 1346, http://dx.doi.org/10.1038/ncomms2336.

Mahrt, E., Agarwal, A., Perkel, D., Portfors, C., Elemans, C.P.H., 2016. Mice produce ultrasonic vocalizations by intra-laryngeal planar impinging jets. Curr. Biol. 26, 1–2, http://dx.doi.org/10.1016/j.cub.2016.08.032.

Maronde, E., Schilling, A.F., Seitz, S., Schinke, T., Schmutz, I., van der Horst, G., Amling, M., Albrecht, U., 2010. The clock genes period 2 and cryptochrome 2 differentially balance bone formation. PLoS One 5, e11527, http://dx.doi.org/10.1371/journal.pone.0011527.g004.

Nishio, T., Bando, H., Bamba, H., Hisa, Y., Okamura, H., 2008. Circadian gene expression in the murine larynx. Auris Nasus Larynx 35, 539–544, http://dx.doi.org/10.1016/j.anl.2007.12.008.

Paulsen, K., 1967. Das Prinzip der Stimmbildung in der Wirbeltierreihe und beim Menschen. Akad. Verl.-Ges., Frankfurt a.M.

Pilorz, V., Steinlechner, S., 2008. Low reproductive success in Per1 and Per2 mutant mouse females due to accelerated ageing? Reproduction 135, 559–568, http://dx.doi.org/10.1530/REP-07-0434.

Pilorz, V., Steinlechner, S., Oster, H., 2009. Age and oestrus cycle-related changes in glucocorticoid excretion and wheel-running activity in female mice carrying mutations in the circadian clock genes Per1 and Per2. Physiol. Behav. 96, 57–63, http://dx.doi.org/10.1016/j.physbeh.2008.08.010.

Rawashdeh, O., Jilg, A., Jedlicka, P., Slawska, J., Thomas, L., Saade, A., Schwarzacher, S.W., Stehle, J.H., 2014. PERIOD1 coordinates hippocampal rhythms and memory processing with daytime. Hippocampus 24, 712–723, http://dx.doi.org/10.1002/hipo.22262.

Rawashdeh, O., Jilg, A., Maronde, E., Fahrenkrug, J., Stehle, J.H., 2016. Period1 gates the circadian modulation of memory-relevant signaling in mouse hippocampus by regulating the nuclear shuttling of the CREB kinase pP90RSK. J. Neurochem. 138, 731–745, http://dx.doi.org/10.1111/jnc.13689.

Riede, T., 2011. Subglottal pressure, tracheal airflow, and intrinsic laryngeal muscle activity during rat ultrasound vocalization. J. Neurophysiol. 106, 2580–2592, http://dx.doi.org/10.1152/jn.00478.2011.

Riede, T., Borgard, H.L., Pasch, B., 2017. Laryngeal airway reconstruction indicates that rodent ultrasonic vocalizations are produced by an edge-tone mechanism. R. Soc. Open Sci. 4, 170976, http://dx.doi.org/10.1098/rsos.170976.

Roberts, L.H., 1975a. The functional anatomy of the rodent larynx in relation to audible and ultrasonic cry production. Zool. J. Linn. Soc. 56, 255–264, http://dx.doi.org/10.1111/j.1096-3642.1975.tb00268.x.

Roberts, L.H., 1975b. Evidence for the laryngeal source of ultrasonic and audible cries of rodents. J. Zool. 175, 243–257, http://dx.doi.org/10.1111/j.1469-7998.1975.tb01399.x.

Roberts, L.H., 1975c. The rodent ultrasound production mechanism. Ultrasonics 13, 83–88, http://dx.doi.org/10.1016/0041-624X(75)90052-9.

Sagartz, J.W., Madarasz, A.J., Forsell, M.A., Burger, G.T., Ayres, P.H., Coggins, C.R.E., 1992. Histological sectioning of the rodent larynx for inhalation toxicity testing. Toxicol. Pathol. 20, 118–121, http://dx.doi.org/10.1177/019262339202000115.

Sanders, I., Weisz, D.J., Yang, B.Y., Fung, K., Abstr, A.A.S.N., n.d. 2001. The Mechanism of Ultrasonic Vocalization in the Rat.

Scattoni, M.L., Crawley, J., Ricceri, L., 2009. Ultrasonic vocalizations: a tool for behavioural phenotyping of mouse models of neurodevelopmental disorders. Neurosci. Biobehav. Rev. 33, 508–515, http://dx.doi.org/10.1016/j.neubiorev.2008.08.003.

Schindelin, J., Arganda-Carreras, I., Frise, E., Kaynig, V., Longair, M., Pietzsch, T., Preibisch, S., Rueden, C., Saalfeld, S., Schmid, B., Tinevez, J.-Y., White, D.J., Hartenstein, V., Eliceiri, K., Tomancak, P., Cardona, A., 2012. Fiji: an open-source platform for biological-image analysis. Nat. Methods 9, 676–682, http://dx.doi.org/10.1038/nmeth.2019.

Takarada, T., Xu, C., Ochi, H., Nakazato, R., Yamada, D., Nakamura, S., Kodama, A., Shimba, S., Mieda, M., Fukasawa, K., Ozaki, K., Iezaki, T., Fujikawa, K., Yoneda, Y., Numano, R., Hida, A., Tei, H., Takeda, S., Hinoi, E., 2017. Bone resorption is regulated by circadian clock in osteoblasts. J. Bone Miner. Res. 32, 872–881, http://dx.doi.org/10.1002/jbmr.3053.

Thomas, L.B., Stemple, J.C., Andreatta, R.D., Andrade, F.H., 2009. Establishing a new animal model for the study of laryngeal biology and disease: an anatomic study of the mouse larynx. J. Speech Lang. Hear. Res. 52, 802–811, http://dx.doi.org/10.1044/1092-4388(2008/08-0087.

Wöhr, M., Schwarting, R.K.W., 2010. Rodent ultrasonic communication and its relevance for models of neuropsychiatric disorders. e-Neuroforum 1, 71–80, http://dx.doi.org/10.1007/s13295-010-0012-z.

Yang, N., Meng, Q.-J., 2016. Circadian clocks in articular cartilage and bone. J. Biol. Rhythms 31, 415–427, http://dx.doi.org/10.1177/0748730416662748.

Yoruk, O., Dane, S., Ucuncu, H., Aktan, B., Can, I., 2009. Stereological evaluation of laryngeal cancers using computed tomography via the cavalieri method: correlation between tumor volume and number of neck lymph node metastases. J. Craniofac. Surg. 20, 1504–1507, http://dx.doi.org/10.1097/SCS.0b013e3181b09bc3.

Zippelius, H.-M., Schleidt, W.M., 1956. Ultraschall-Laute bei jungen Mäusen. Naturwissenschaften 43, 502.